Stable Multiring and Rotating Solitons in Two-Dimensional Spin-Orbit-Coupled Bose-Einstein Condensates with a Radially Periodic Potential

Yaroslav V. Kartashov[1,2] and Dmitry A. Zezyulin[3]

[1]*ICFO–Institut de Ciencies Fotoniques, The Barcelona Institute of Science and Technology,*
08860 Castelldefels (Barcelona), Spain
[2]*Institute of Spectroscopy, Russian Academy of Sciences, Troitsk, Moscow, 108840, Russia*
[3]*ITMO University, St. Petersburg 197101, Russia*

We consider two-dimensional spin-orbit-coupled atomic Bose-Einstein condensate in a radially periodic potential. The system supports different types of stable self-sustained states including radially symmetric vorticity-carrying modes with different topological charges in two spinor components that may have multiring profiles and at the same time remain remarkably stable for repulsive interactions. Solitons of the second type show persistent rotation with constant angular frequency. They can be stable for both repulsive and attractive interatomic interactions. Because of the inequivalence between clockwise and counterclockwise rotation directions introduced by spin-orbit coupling, the properties of such solitons strongly differ for positive and negative rotation frequencies. The collision of solitons located in the same or different rings is accompanied by a change of the rotation frequency that depends on the phase difference between colliding solitons.

Nonlinear wave phenomena in atomic Bose-Einstein condensates (BECs) attract considerable attention [1–3]. Depending on the sign of the interatomic interactions, one can observe the formation in BECs of bright or dark solitons. Their properties critically depend on the dimensionality of the condensate, since multidimensional states in BECs with attractive and repulsive interatomic interactions may be prone, respectively, to collapse or various snaking instabilities. Bright solitons can be obtained in a Bose-Fermi mixture of degenerate gases, even if interatomic interactions in the Bose component are repulsive [4,5]. Another powerful approach to stabilization of multidimensional states in BECs relies on the external potentials, including periodic ones [6–8]. Besides conventional states that do not change upon evolution [9], such potentials, when they are radially symmetric [10–12], support stable solitons exhibiting persistent rotation. The properties of such solitons in single-component BECs do not depend on the rotation direction.

This situation may change dramatically in spin-orbit-coupled two-component condensates (SO BECs), which are attracting steadily growing interest. SO BECs, representing a mixture of different states of the same atomic species, were recently used for demonstration of coupling between pseudospin degrees of freedom and spatial structure of the condensate [13–15]. SO BECs offer a versatile platform for investigation of the nonlinear phenomena in the presence of synthetic fields [16] and gauge potentials [17]; see Ref. [18] for a review. SO coupling notably modifies dispersion of the system [19,20], it may break

Galilean invariance [14,21], and it substantially impacts properties of one- [22,23] and multidimensional [24,25] solitons in the free space. Especially intriguing is the impact of SO coupling on BEC in the external potentials, where possible symmetries of self-sustained states and their evolution dynamics are determined by the symmetry of the potential. It was studied for solitons on a ring [26] and in harmonic trap [27], in toroidal traps [28], Bessel [29], and periodic [30] lattices.

While it was shown for radially symmetric potentials [28] that SO coupling notably enriches two-dimensional soliton families and leads to the appearance of azimuthal density modulations, the most important and unexpected manifestation of this effect, consisting in the breakup of equivalence of two rotation directions (clockwise and counterclockwise) for solitons, was not demonstrated in atomic BECs. This is also the case for literature [31] on trapped SO BECs under rotation that studies condensate transformation for one sign of the rotation frequency. While this inequivalence has been encountered in polariton condensates in a circular geometry [32], polaritons represent an essentially nonequilibrium system, where dominating interactions are repulsive, and where effective SO coupling has a completely different physical origin (it stems from TE-TM splitting) and is relatively weak. Thus, the question arises of whether this phenomenon exists in conservative atomic BECs where SO coupling is considerable and where interactions can be both repulsive and attractive.

Here we first introduce SO coupling into BECs in a radially periodic potential and show that in the repulsive

case it supports stable multiring vortex solitons carrying different topological charges in two components. Such structures have never been obtained in SO BECs before and are in clear contrast to previously encountered azimuthally modulated patterns. Second, we show that radially periodic potentials support stable rotating multipole states for repulsive nonlinearity and crescentlike fundamental states for attractive nonlinearity, reminiscent of azimuthons [33], that feature unexpected dependence not only on modulus, but also on sign of the rotation frequency, clearly illustrating inequivalence of two azimuthal directions. Third, we study interactions of rotating solitons for attractive nonlinearity and show that they lead to change in rotation frequency that also depends on soliton phase difference.

Mean-field dynamics of two-dimensional BECs is described by the normalized Gross-Pitaevskii equations with Rashba SO coupling [34]:

$$i\partial_t \psi_\pm = -(1/2)(\partial_x^2 + \partial_y^2)\psi_\pm + V(r)\psi_\pm \pm \beta(\partial_x \mp i\partial_y)\psi_\mp$$
$$+ \sigma(|\psi_\pm|^2 + |\psi_\mp|^2)\psi_\pm. \quad (1)$$

Here $(\psi_+, \psi_-)^T$ is the spinor macroscopic wave function, t and x, y are dimensionless time and spatial coordinates, scaled to characteristic time $\hbar/\mathcal{E}_0$ and spatial scale R_0, respectively, $\mathcal{E}_0 = \hbar^2/mR_0^2$ is characteristic energy, m is the atomic mass, β characterizes the strength of SO coupling that can be considerable, $\sigma = \pm 1$ corresponds to repulsive or attractive interactions, $V(r) = 2V_0\cos^2(r)$ is the radially periodic potential with depth $2V_0$ measured in units of $\mathcal{E}_0$ (hereafter r and θ are the polar radius and angle); in what follows, we set $V_0 = 3$. The radially periodic potential can be created using a cylindrical laser beam whose amplitude is modulated with a patterned mask (the conical diffraction of the beam with the waist diameter $\simeq 100 \ \mu$m will be negligible for the tightly confined disk-shaped condensate with thickness $\simeq 2 \ \mu$m [12]). SO coupling is created by laser beams which couple different states of ^{87}Rb atoms (the case of repulsive interactions) or ^{7}Li atoms (attractive interactions); its strength can be varied in a broad range depending on laser configurations [20]; see also Refs. [13–15,22] for detailed discussion on implementation of SO BECs.

The simplest states are radially symmetric solitons $\psi_\pm = u_\pm(r)e^{-i\mu t + im_\pm \theta}$, where $m_\pm$ are the topological charges satisfying the condition $m_- = m_+ + 1$ that is due to the linear spin-orbit coupling preserving the total angular momentum, μ is the chemical potential, and $u_\pm$ are real valued. We search for localized solutions carrying finite norm $N = 2\pi \int_0^\infty r(u_+^2 + u_-^2)dr$ (which is proportional to the total number of particles in the condensate). At $r \to \infty$ the effect of nonlinear terms becomes negligible, and the intervals of chemical potential, where localized states can exist, are determined by the eigenvalue problem $\mu u_\pm = -(1/2)\partial_r^2 u_\pm + V(r)u_\pm \pm \beta\partial_r u_\mp$.
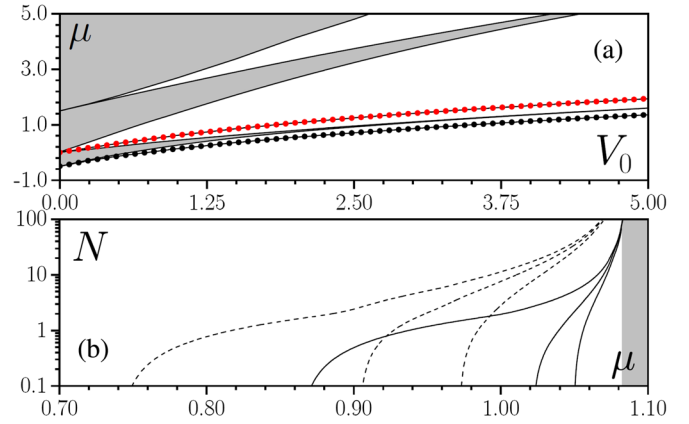
FIG. 1. (a) Bands (gray) and gaps (white) of radial potential and eigenvalues of linear modes (lines with circles) with $m_\pm = (-1, 0)$ residing in the first potential minimum. (b) N versus μ for simplest soliton families with $m_\pm = (-1, 0)$ (solid lines) and $m_\pm = (-2, -1)$ (dashed lines) in the semi-infinite gap at $\sigma = 1$. For each $m_\pm$ set three families are shown with density maxima in the first, second, and third minima of $V(r)$.

This problem is π periodic and features the band gap spectrum shown in Fig. 1(a). Localized nonlinear modes—radial gap solitons—exist for μ values lying in the spectral gaps [white regions in Fig. 1(a)]. However, in contrast to usual gap solitons, nonlinear modes in the radially periodic potential remain completely localized also in the small-amplitude limit, when the corresponding norm vanishes, $N \to 0$. This feature is readily visible from Fig. 1(b), where we plot several dependencies $N(\mu)$ for nonlinear modes with topological charges $m_\pm = (-1, 0)$ (solid curves) and $m_\pm = (-2, -1)$ (dashed curves) and density maxima located in radial minima of the potential at $r = \pi/2$, $3\pi/2$, and $5\pi/2$. In the limit $N \to 0$, each of these soliton families bifurcates from appropriate localized linear mode with chemical potential μ from the gap. Eigenvalues of linear modes in the semi-infinite and first finite gaps from which the simplest solitons with density maximum at $r = \pi/2$ bifurcate are shown in Fig. 1(a) by lines with circles. In spite of the repulsive interactions, $\sigma = 1$, families shown in Fig. 1(b) belong to the semi-infinite gap (which is possible due to the radial periodicity of the trap). When μ approaches the edge of the gap, vortex modes acquire well-pronounced multiring structure (see examples in Fig. 2). Standard linear stability analysis [34,36] and direct integration of Eq. (1) indicate stability of all vortex states shown in Figs. 1(b) and 2, in spite of their complex multiring shapes. Stable radially symmetric vortex solitons can be found not only in the semi-infinite gap but also in finite spectral gaps, as shown in Figs. 3 and 5.

Now we turn to rotating states without radial symmetry. They are sought as $\psi_\pm = u_\pm(x', y')e^{-i(\mu \pm \omega/2)t}$ in the rotating frame $x' = x\cos(\omega t) + y\sin(\omega t)$, $y' = y\cos(\omega t) - x\sin(\omega t)$, where complex functions $u_\pm$ solve (we further omit primes)
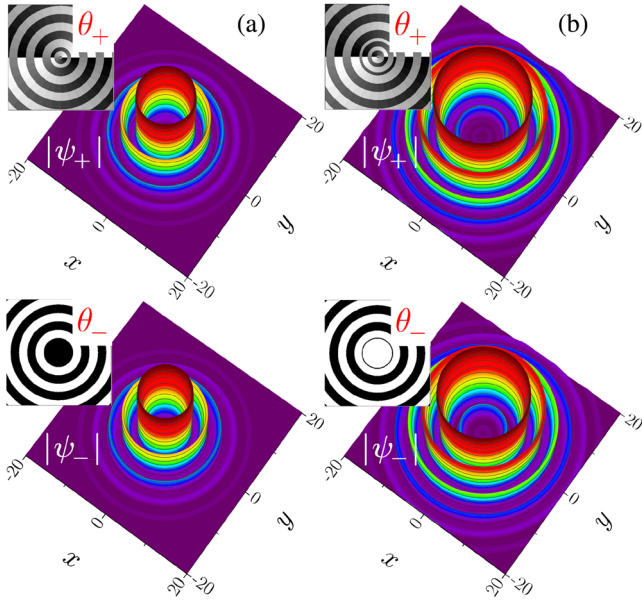
FIG. 2. Modulus and phase (insets) distributions in $m_{\pm} = (-1, 0)$ radially symmetric solitons from different families, with $\mu = 1.05$ (a) and $\mu = 1.06$ (b) at $\beta = 1$, $\sigma = 1$.

$$\mu u_{\pm} = -(1/2)(\partial_x^2 + \partial_y^2)u_{\pm} + V(r)u_{\pm} \pm \beta(\partial_x \mp i\partial_y)u_{\mp}$$
$$+ \sigma(|u_{\pm}|^2 + |u_{\mp}|^2)u_{\pm} + i\omega(x\partial_y - y\partial_x)u_{\pm}$$
$$\mp (\omega/2)u_{\pm}. \qquad (2)$$

Rotation with frequency ω results in the penultimate Coriolis term in Eq. (2), while the last term originates from the assumed form of time dependence in $\psi_{\pm}$ that is required to eliminate time dependence in the SO-coupling term in the rotating frame. Equation (2) admits a variety of rotating solitons residing in different radial minima of the potential. We start with repulsive nonlinearity ($\sigma = 1$) and consider the simplest solitons from the first minimum at $r = \pi/2$ with chemical potentials μ from the first finite gap. At $\beta, \omega = 0$, they represent dipole (two out-of-phase spots in the u_+ or u_- component) and quadrupole (four spots in u_+ or u_- with π phase jumps) solitons. At $\beta = 0$, increasing or decreasing rotation frequency smoothly transforms multipole states into radially symmetric vortices. The dependence of amplitude $a_{\pm} = \max |u_{\pm}(x, y)|$ of soliton components on ω is symmetric in this case; see line with open circles in Fig. 3(a) for dipole solitons. Thus, at $\beta = 0$ the properties of such solitons do not depend on the rotation direction. This picture changes qualitatively in the presence of SO coupling: the dependence $a_{\pm}(\omega)$ becomes asymmetric at $\beta \neq 0$. For dipole solitons with a dominating u_+ component, the entire domain of existence of rotating solitons shifts toward positive frequency values [lines with solid circles in Fig. 3(a) between two vertical dashed lines marking the border of the existence domain]. For dipole states with a dominating u_- component, the existence domain shifts toward negative frequencies. The existence domains for rotating solitons with different dominating components are
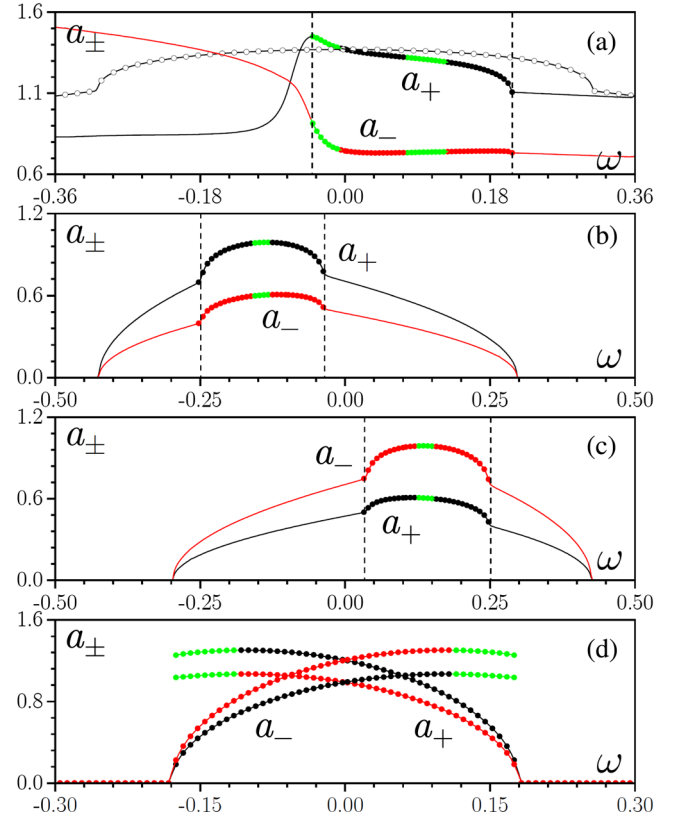
FIG. 3. Lines with solid circles show amplitudes $a_{\pm}$ of $\psi_{\pm}$ components in rotating dipole (a) and quadrupole (b),(c) solitons versus ω at $\mu = 3$, $\beta = 0.5$, $\sigma = 1$. Line with open circles in (a) shows $a_+(\omega)$ dependence at $\beta = 0$. Dominating component is ψ_+ in (b) and ψ_- in (c). Thin lines in (b) and (c) correspond to radially symmetric states. (d) $a_{\pm}(\omega)$ in rotating fundamental solitons at $\mu = 0.6$, $\beta = 0.5$, $\sigma = -1$. Green circles indicate unstable branches.

thus mirror symmetric with respect to $\omega = 0$, as illustrated for quadrupole solitons in Figs. 3(b) and 3(c). Inequivalence of azimuthal directions in SO BECs illustrated by Fig. 3 is one of the central results of this Letter. For a characteristic scale of $R_0 = 2 \ \mu m$, dimensionless frequency $\omega = 0.25$ corresponds to rotation periods of 137 ms in ^{87}Rb and 11 ms in ^{7}Li condensate [34], that is well below the condensate lifetime available in the state-of-the-art experiments.

Variation of rotation frequency causes notable shape transformations. Examples of modulus $|\psi_{\pm}|$ and phase $\theta_{\pm}$ distributions for different frequencies in dipole and quadrupole solitons are shown in Figs. 4(a)–4(d). On the right-hand edge of the existence domain in ω [Fig. 4(a)], such dipoles turn into $m_{\pm} = (-1, 0)$ radially symmetric vortices, while on the left-hand edge [Fig. 4(b)] they become strongly modulated and dynamically unstable. Quadrupole solitons transform into $m_{\pm} = (-2, -1)$ vortices on the right-hand edge [Fig. 4(c)] of the existence domain and into $m_{\pm} = (+2, +3)$ vortices on its left-hand edge [Fig. 4(d)]. Transformation of phase distribution upon variation of ω resembles topological charge flipping [37].
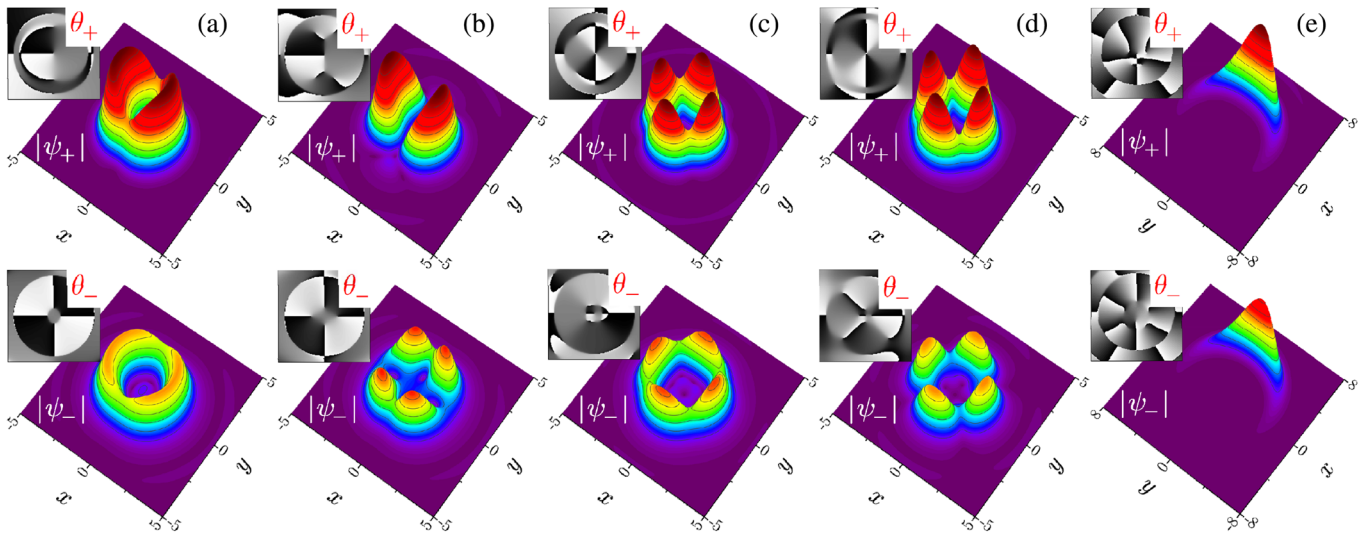
FIG. 4. Modulus and phase (insets) distributions in dipole solitons with (a) $\omega = 0.13$, (b) $\omega = -0.04$, and quadrupole solitons with (c) $\omega = -0.06$, (d) $\omega = -0.22$ at $\mu = 3$, $\beta = 0.5$, $\sigma = 1$, and fundamental solitons with (e) $\omega = 0.15$ at $\mu = 0.6$, $\beta = 0.5$, $\sigma = -1$. In all cases ψ_+ is a dominating component; $|\psi_+|$ and $|\psi_-|$ distributions are plotted with the same scale in each soliton.

Families of radially symmetric states into which rotating solitons transform can be further continued in ω, as shown by thin lines in Fig. 3. At fixed ω and $\sigma = 1$, all rotating solitons (lines with circles) bifurcate with increase of chemical potential μ from radially symmetric solitons (thin lines), which emanate from corresponding linear modes, as shown in Fig. 5. The charge of the state, from which bifurcation occurs, is determined by ω: it is $(-1, 0)$ in Fig. 5(a) and $(-2, -1)$ in Fig. 5(b). When μ increases and approaches the border of the first gap, rotating modes develop multiring structure and eventually delocalize.

In contrast to polariton condensates, both dipole and quadrupole rotating solitons in repulsive SO BECs are dynamically stable in wide parameter regions even for β values comparable to 1. Stability was also tested by

modeling the evolution of slightly perturbed states up to huge times $t \sim 10^4$ in Eq. (1). Instability domains are indicated by green circles in Figs. 3 and 5, while black or red circles correspond to stable branches. Rotating solitons are always stable in the parameter domains adjacent to bifurcation points from radially symmetric solitons. Examples of evolutions with stable and unstable rotations are given in Figs. 6(a)–6(c).

SO BECs with attractive nonlinearity $(\sigma = -1)$ support simpler fundamental rotating solitons with unusual crescentlike shapes; see Fig. 4(e). Such solitons exist in

FIG. 5. Lines with circles show $a_\pm(\mu)$ dependencies for (a) rotating dipole soliton with $\omega = 0.12$ and (b) quadrupole soliton with $\omega = -0.06$ at $\beta = 0.5$, $\sigma = 1$. Thin lines show $a_\pm(\mu)$ for radially symmetric $m_\pm = (-1, 0)$ (a) and $m_\pm = (-2, -1)$ (b) states. Green circles indicate unstable branches.
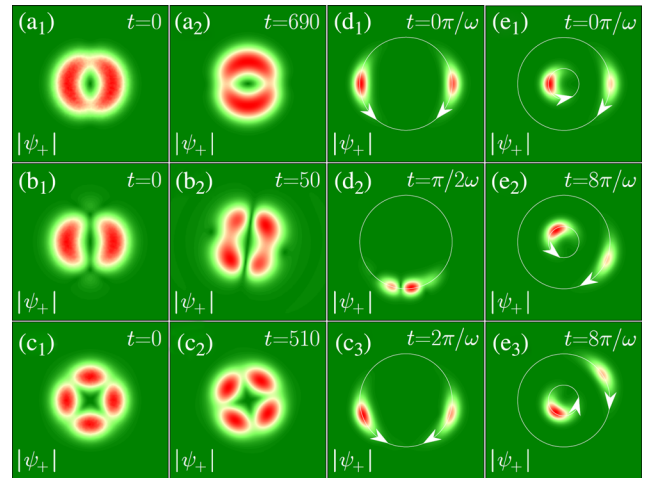
FIG. 6. Stable (a),(c) and unstable (b) evolution of rotating dipole and quadrupole solitons at (a) $\omega = 0.13$, (b) $\omega = -0.04$, (c) $\omega = -0.22$ and $\mu = 3$, $\beta = 0.5$, $\sigma = 1$. Interaction of two fundamental solitons in the same (d1)–(d3) and in different (e1)–(e3) rings at $\mu = 0.6$, $\beta = 0.5$, $\sigma = -1$. Solitons are in phase in (d1)–(d3) and (e2) and out of phase in (e3) and have opposite rotation frequencies $\omega = \pm 1$.

a semi-infinite gap and resemble whispering-gallery modes [38]. The dependencies of amplitudes $a_{\pm}$ of such solitons are also strongly asymmetric in rotation frequency ω [Fig. 3(d)]: at one border of the existence domain in ω soliton gradually expands along the entire ring where it resides (soliton is stable in broad domain adjacent to this border), while on another border one observes development of an unstable multiring structure. Since such solitons are better localized than their counterparts in repulsive condensate, one can study their collision in the same [Figs. 6(d1)–6(d3)] or in different [Figs. 6(e1)–6(e3)] rings. Taking two solitons with opposite rotation frequencies ω and equal norms (μ values), one unexpectedly finds that after collision [Fig. 6(d2)] both solitons accelerate [compare input in Fig. 6(d1) with output in Fig. 6(d3) after $t = 2\pi/\omega$]; i.e., collision in this system changes rotation frequencies. Moreover, the variation in ω depends on the phase difference between colliding solitons. Thus, when two solitons with opposite frequencies at $t = 0$ collide in different rings [Figs. 6(e1)–6(e3)], the outer (inner) soliton accelerates (decelerates) upon consecutive collisions for in-phase solitons [Fig. 6(e2)], while for out-of-phase states this tendency reverses [Fig. 6(e3)], leading to different final density distributions.

In summary, we demonstrated that SO coupling in trapped BECs with repulsive or attractive interaction breaks the equivalence of two rotation directions. Rotating solitons feature strongly asymmetric existence domains in rotation frequency and feature nonconventional collisional behaviors involving their acceleration or deceleration determined by the phase difference between solitons.

[1] C. Pethick and H. Smith, *Bose-Einstein Condensation in Dilute Gases* (Cambridge University Press, Cambridge, England, 2002); L. Pitaevskii and S. Stringari, *Bose-Einstein Condensation* (Clarendon Press, Oxford, 2003).

[2] *Emergent Nonlinear Phenomena in Bose-Einstein Condensates*, edited by P. G. Kevrekidis, D. J. Frantzeskakis, and R. Carretero-González, Springer Series on Atomic, Optical, and Plasma Physics Vol. 45 (Springer, New York, 2008).

[3] A. L. Fetter, Rotating trapped Bose-Einstein condensates, Rev. Mod. Phys. **81**, 647 (2009).

[4] T. Karpiuk, M. Brewczyk, S. Ospelkaus-Schwarzer, K. Bongs, M. Gajda, and K. Rzążewski, Soliton Trains in Bose-Fermi Mixtures, Phys. Rev. Lett. **93**, 100401 (2004); J. Santhanam, V. M. Kenkre, and V. V. Konotop, Solitons of Bose-Fermi mixtures in a strongly elongated trap, Phys. Rev. A **73**, 013612 (2006).

[5] B. J. DeSalvo, K. Patel, G. Cai, and C. Chin, Fermion-mediated interactions between bosonic atoms, arXiv:1808.07856.

[6] V. A. Brazhnyi and V. V. Konotop, Theory of nonlinear matter waves in optical lattices, Mod. Phys. Lett. B **18**, 627 (2004); Y. V. Kartashov, B. A. Malomed, and L. Torner, Solitons in nonlinear lattices, Rev. Mod. Phys. **83**, 247 (2011).

[7] O. Morsch and M. Oberthaler, Dynamics of Bose-Einstein condensates in optical lattices, Rev. Mod. Phys. **78**, 179 (2006).

[8] R. Carretero-González, D. J. Frantzeskakis, and P. G. Kevrekidis, Nonlinear waves in Bose-Einstein condensates: Physical relevance and mathematical techniques, Nonlinearity **21**, R139 (2008).

[9] E. A. Ostrovskaya and Y. S. Kivshar, Matter-Wave Gap Solitons in Atomic Band-Gap Structures, Phys. Rev. Lett. **90**, 160407 (2003); B. Eiermann, T. Anker, M. Albiez, M. Taglieber, P. Treutlein, K.-P. Marzlin, and M. K. Oberthaler, Bright Bose-Einstein Gap Solitons of Atoms with Repulsive Interaction, Phys. Rev. Lett. **92**, 230401 (2004); E. A. Ostrovskaya and Y. S. Kivshar, Matter-Wave Gap Vortices in Optical Lattices, Phys. Rev. Lett. **93**, 160405 (2004).

[10] Y. V. Kartashov, V. A. Vysloukh, and L. Torner, Rotary Solitons in Bessel Optical Lattices, Phys. Rev. Lett. **93**, 093904 (2004); Stable Ring-Profile Vortex Solitons in Bessel Optical Lattices, Phys. Rev. Lett. **94**, 043902 (2005); X. S. Wang, Z. G. Chen, and P. G. Kevrekidis, Observation of Discrete Solitons and Soliton Rotation in Optically Induced Periodic Ring Lattices, Phys. Rev. Lett. **96**, 083904 (2006).

[11] A. V. Carpentier and H. Michinel, A ring accelerator for matter-wave solitons, Europhys. Lett. **78**, 10002 (2007); C. Ryu, M. F. Andersen, P. Clade, V. Natarajan, K. Helmerson, and W. D. Phillips, Observation of Persistent Flow of a Bose-Einstein Condensate in a Toroidal Trap, Phys. Rev. Lett. **99**, 260401 (2007).

[12] B. Baizakov, B. A. Malomed, and M. Salerno, Matter-wave solitons in radially periodic potentials, Phys. Rev. E **74**, 066615 (2006).

[13] Y. J. Lin, K. Jiménez-García, and I. B. Spielman, Spin-orbit-coupled Bose-Einstein condensates, Nature (London) **471**, 83 (2011).

[14] C. Hamner, Y. Zhang, M. A. Khamehchi, M. J. Davis, and P. Engels, Spin-Orbit-Coupled Bose-Einstein Condensates in a One-Dimensional Optical Lattice, Phys. Rev. Lett. **114**, 070401 (2015).

[15] Z. Wu, L. Zhang, W. Sun, X. T. Xu, B. Z. Wang, S. C. Ji, Y. Deng, S. Chen, X. J. Liu, and J. W. Pan, Realization of two-dimensional spin-orbit coupling for Bose-Einstein condensates, Science **354**, 83 (2016).

[16] Y.-J. Lin, R. L. Compton, K. Jiménez-García, J. V. Porto, and I. B. Spielman, Synthetic magnetic fields for ultracold neutral atoms, Nature (London) **462**, 628 (2009).

[17] J. Ruseckas, G. Juzeliūnas, P. Öhberg, and M. Fleischhauer, Non-Abelian Gauge Potentials for Ultracold Atoms with Degenerate Dark States, Phys. Rev. Lett. **95**, 010404 (2005); T.-L. Ho and S. Zhang, Bose-Einstein Condensates with Spin-Orbit Interaction, Phys. Rev. Lett. **107**, 150403 (2011); Y.-J. Lin, R. L. Compton, A. R. Perry, W. D. Phillips, J. V. Porto, and I. B. Spielman, Bose-Einstein Condensate in a

Uniform Light-Induced Vector Potential, Phys. Rev. Lett. **102,** 130401 (2009).

[18] J. Dalibard, F. Gerbier, G. Juzeliūnas, and P. Öhberg, Colloquium: Artificial gauge potentials for neutral atoms, Rev. Mod. Phys. **83,** 1523 (2011).

[19] C. Wang, C. Gao, C.-M. Jian, H. Zhai, C. Wang, C. Gao, C.-M. Jian, and H. Zhai, Spin-Orbit Coupled Spinor Bose-Einstein Condensates, Phys. Rev. Lett. **105,** 160403 (2010); S. Sinha, R. Nath, and L. Santos, Trapped Two-Dimensional Condensates with Synthetic Spin-Orbit Coupling, Phys. Rev. Lett. **107,** 270401 (2011); H. Hu, B. Ramachandhran, H. Pu, and X.-J. Liu, Spin-Orbit Coupled Weakly Interacting Bose-Einstein Condensates in Harmonic Traps, Phys. Rev. Lett. **108,** 010402 (2012); Y. Li, G. I. Martone, L. P. Pitaevskii, and S. Stringari, Superstripes and the Excitation Spectrum of a Spin-Orbit-Coupled Bose-Einstein Condensate, Phys. Rev. Lett. **110,** 235302 (2013).

[20] Y. Zhang, L. Mao, and C. Zhang, Mean-Field Dynamics of Spin-Orbit-Coupled Bose-Einstein Condensates, Phys. Rev. Lett. **108,** 035302 (2012).

[21] Q. Zhu, C. Zhang, and B. Wu, Exotic superfluidity in spin-orbit coupled Bose-Einstein condensates, Europhys. Lett. **100,** 50003 (2012).

[22] V. Achilleos, D. J. Frantzeskakis, P. G. Kevrekidis, and D. E. Pelinovsky, Matter-Wave Bright Solitons in Spin-Orbit Coupled Bose-Einstein Condensates, Phys. Rev. Lett. **110,** 264101 (2013).

[23] Y. Xu, Y. Zhang, and B. Wu, Bright solitons in spin-orbit-coupled Bose-Einstein condensates, Phys. Rev. A **87,** 013614 (2013); Y. V. Kartashov, V. V. Konotop, and D. A. Zezyulin, Bose-Einstein condensates with localized spin-orbit coupling: Soliton complexes and spinor dynamics, Phys. Rev. A **90,** 063621 (2014).

[24] H. Sakaguchi, B. Li, and B. A. Malomed, Creation of two-dimensional composite solitons in spin-orbit-coupled self-attractive Bose–Einstein condensates in free space, Phys. Rev. E **89,** 032920 (2014); X. Jiang, Z. Fan, Z. Chen, W. Pang, Y. Li, and B. A. Malomed, Two-dimensional solitons in dipolar Bose-Einstein condensates with spin-orbit coupling, Phys. Rev. A **93,** 023633 (2016).

[25] Y.-C. Zhang, Z.-W. Zhou, B. A. Malomed, and H. Pu, Stable Solitons in Three-Dimensional Free Space without the Ground State: Self-Trapped Bose-Einstein Condensates with Spin-Orbit Coupling, Phys. Rev. Lett. **115,** 253902 (2015).

[26] O. Fialko, J. Brand, and U. Zülicke, Soliton magnetization dynamics in spin-orbit-coupled Bose-Einstein condensates, Phys. Rev. A **85,** 051605(R) (2012).

[27] D. A. Zezyulin, R. Driben, V. V Konotop, and B. A. Malomed, Nonlinear modes in binary bosonic condensates with pseudo-spin-orbital coupling, Phys. Rev. A **88,** 013607 (2013).

[28] E. Ö. Karabulut, F. Malet, A. L. Fetter, G. M. Kavoulakis, and S. M. Reimann, Spin-orbit-coupled Bose-Einstein-condensed atoms confined in annular potentials, New J. Phys. **18,** 015013 (2016); X.-F. Zhang, M. Kato, W. Han, S.-G. Zhang, and H. Saito, Spin-orbit-coupled Bose–Einstein condensates held under a toroidal trap, Phys. Rev. A **95,** 033620 (2017); A. C. White, Y. Zhang, and T. Busch, Odd-petal-number states and persistent flows in spin-orbit-coupled Bose-Einstein condensates, Phys. Rev. A **95,** 041604(R) (2017).

[29] H. Li, S.-L. Xu, M. R. Belić, and J.-X. Cheng, Three-dimensional solitons in Bose–Einstein condensates with spin-orbit coupling and Bessel optical lattices, Phys. Rev. A **98,** 033827 (2018).

[30] Y. V. Kartashov, V. V. Konotop, and F. Kh. Abdullaev, Gap Solitons in a Spin-Orbit-Coupled Bose-Einstein Condensate, Phys. Rev. Lett. **111,** 060402 (2013); V. E. Lobanov, Y. V. Kartashov, and V. V. Konotop, Fundamental, Multipole, and Half-Vortex Gap Solitons in Spin-Orbit Coupled Bose-Einstein Condensates, Phys. Rev. Lett. **112,** 180403 (2014); Y. Zhang, Y. Xu, and T. Busch, Gap solitons in spin-orbit-coupled Bose-Einstein condensates in optical lattices, Phys. Rev. A **91,** 043629 (2015); M. Salerno, F. Kh. Abdullaev, G. A. Gammal, and L. Tomio, Tunable spin-orbit-coupled Bose–Einstein condensates in deep optical lattices, Phys. Rev. A **94,** 043602 (2016).

[31] X.-Qi. Xu and J. H. Han, Spin-Orbit Coupled Bose-Einstein Condensate under Rotation, Phys. Rev. Lett. **107,** 200401 (2011); J. Radić, T. A. Sedrakyan, I. B. Spielman, and V. Galitski, Vortices in spin-orbit-coupled Bose-Einstein condensates, Phys. Rev. A **84,** 063604 (2011); X.-F. Zhou, J. Zhou, and C. Wu, Vortex structures of rotating spin-orbit-coupled Bose-Einstein condensates, Phys. Rev. A **84,** 063624 (2011); H. Sakaguchi and K. Umeda, Solitons and vortex lattices in the gross-pitaevskii equation with spin-orbit coupling under rotation, J. Phys. Soc. Jpn. **85,** 064402 (2016); J.-G. Wang, L.-L. Xu, and S.-J. Yang, Ground-state phases of a rotating spin-orbit-coupled Bose-Einstein condensate in an optical lattice, Europhys. Lett. **120,** 20006 (2017); Z.-M. He, X.-F. Zhang, M. Kato, W. Han, and H. Saito, Stationary states and rotational properties of spin-orbit-coupled Bose-Einstein condensates held under a toroidal trap, Phys. Lett. A **382,** 1690 (2018).

[32] D. A. Zezyulin, Y. V. Kartashov, D. V. Skryabin, and I. A. Shelykh, Spin-orbit coupled polariton condensates in a radially periodic potential: Multiring vortices and rotating solitons, ACS Photonics **5,** 3634 (2018).

[33] A. S. Desyatnikov, A. A. Sukhorukov, and Y. S. Kivshar, Azimuthons: Spatially Modulated Vortex Solitons, Phys. Rev. Lett. **95,** 203904 (2005); V. M. Lashkin, Two-dimensional multisolitons and azimuthons in Bose-Einstein condensates, Phys. Rev. A **77,** 025602 (2008).

[34] See Supplemental Material at http://link.aps.org/supplemental/10.1103/PhysRevLett.122.123201 for the Gross-Pitaesvkii equation written in physical units and details of stability analysis, which includes Ref. [35].

[35] L. D. Carr, M. J. Holland, and B. A. Malomed, Macroscopic quantum tunnelling of Bose-Einstein condensates in a finite potential well, J. Phys. B **38,** 3217 (2005).

[36] A. L. Fetter and A. A. Svidzinsky, Vortices in a trapped dilute Bose-Einstein condensate, J. Phys. Condens. Matter **13,** R135 (2001).

[37] A. Bezryadina, D. N. Neshev, A. S. Desyatnikov, J. Young, Z. Chen, and Y. S. Kivshar, Observation of topological transformations of optical vortices in two-dimensional photonic lattices, Opt. Express **14,** 8317 (2006).

[38] T. J. Kippenberg, A. L. Gaeta, M. Lipson, and M. L. Gorodetsky, Dissipative Kerr solitons in optical micro-cavities, Science **361,** eaan8083 (2018); C. P. Jisha, Y. Y. Lin, T. D. Lee, and R. K. Lee, Crescent Waves in Optical Cavities, Phys. Rev. Lett. **107,** 183902 (2011).